Acta Cryst. (1999). B**55**, 917–922

Electron density study of $KNiF_3$ by the vacuum-camera-imaging plate method

Elizabeth A. Zhurova,[a]† Vladimir V. Zhurov[b] and Kiyoaki Tanaka[c]*

[a]*CREST, Japanese Science and Technology Corporation, Nagoya Institute of Technology, Gokiso-cho, Showa-ku, Nagoya 466, Japan,* [b]*Karpov' Institute of Physical Chemistry, ul. Vorontsovo pole 10, 103064 Moscow, Russia, and* [c]*Nagoya Institute of Technology, Gokiso-cho, Showa-ku, Nagoya 466, Japan. E-mail: kiyo@tana1.kyy.nitech.ac.jp*

(*Received 24 February 1999; accepted 28 June 1999*)

Abstract

The electron density measurements of $KNiF_3$, nickel potassium trifluoride, by the vacuum-camera-imaging plate (VCIP) method and using a four-circle diffractometer with scintillation counter, are performed and compared. In the IP (imaging plate) case evacuation allowed the background around peaks to be reduced 50 times, which significantly increased the accuracy of the data, especially for high-angle reflections. A new *VIIPP* program for visualizing and integration of IP data was designed to treat the data, in which the correction for oblique incidence was applied. The resulting electron density reproduces all the features of the accurate conventional measurement.

1. Introduction

The imaging plate (IP; Amemiya & Miyahara, 1988) is becoming more and more popular in crystal structure investigations, especially for macromolecular (*e.g.* Sakabe, 1991; Iversen *et al.*, 1998), organic (Iwasaki *et al.*, 1995) and organometallic (Carducci *et al.*, 1997) compounds. Some new technical devices (Darovsky & Coppens, 1998) and novel integration methods (Bolotovsky *et al.*, 1995) have already been developed to improve the quality of the data obtained with this method. However, the relatively high level of background, which is accumulated during all the exposure time, still remains as one of the important problems of this method. A simple vacuum camera (Tanaka *et al.*, 1999), which allows significant reduction in air scattering, was designed to solve this problem. The vacuum camera was designed to be installed on a conventional four-circle diffractometer to reduce the cost for construction. Single crystal intensity measurements were already carried out *in vacuo* for investigations of very small samples (Ohsumi *et al.*, 1991; Ohsumi *et al.*, 1995), placing the whole diffractometer in an evacuated box. In the present work we report the results of the first accurate IP measurement of electron density in an inorganic compound using the vacuum camera. We compare these results with those from the very precise measurement using the usual four-circle geometry, especially performed for this case. We term the present measurement with the vacuum camera as the Vacuum-Camera-Imaging Plate (VCIP) method.

2. Experimental

For both measurements the same spherical specimen of $KNiF_3$ was employed. It was treated in HNO_3 acid in order to avoid powder rings appearing on the IP from the damaged surface of the sample. It was glued on a lithium borate glass stick with a diameter of 40 μm to reduce the background. The crystal diameter (68 μm) was measured by taking photographs of the specimen with a scale of 2 μm × 400 under a microscope.

For the IP experiment we used the cylindrical vacuum camera (diameter 110 mm and height 90 mm), designed by one of the authors (KT). The detailed construction will be published elsewhere (Tanaka *et al.*, 1999). IPs were positioned on the cylindrical internal surface of the camera and kept in position using a pressing ring. A Fuji BAS-2500 scanner with 50 × 50 μm pixel resolution was used for the intensity readings. Owing to IP saturation, two different sets of measurements with exposure times 8 min and 2 h were performed in order to obtain good statistics for all the reflections. Intensities recorded on an IP decay rapidly in the first 15 min and then fade slowly with time (Amemiya, 1999). Therefore, we waited for 60 min before reading the IP with the scanner to avoid the error owing to fading during the intensity reading over a few minutes. The error is estimated to be less than 1% (Amemiya, 1999). The scan speed was 2° min^{-1} for 8 min images and 1° min^{-1} for 2 h images. All the measurements were performed at room temperature. Evacuation of the camera was performed up to 70 mTorr in 1 h. A collimater and a crystal rotation axis sealed by o-rings are the main reasons for such a long evacuation time, which will be shortened when a diffractometer especially designed for a vacuum camera is constructed. The average background level per pixel was ∼1–3 impulses for 8 min images and 20–30 impulses for 2 h images at high angles. Without evacuation the background is accumulated along the directions parallel

† Permanent address: Institute of Crystallography, Russian Academy of Sciences, Leninsky pr. 59, 117333 Moscow, Russia.

and antiparallel to the incident beam. After evacuation the background level was 50 times less at high angle and 10–20 times less at low angle, where scattering by the crystal and the thin glass stick supporting it was large. The extremely low background at high angles enables us to see reflections near $2\theta = 150^\circ$ (Mo $K\alpha$) more clearly. The vacuum camera was designed so that the primary beam can pass through it to prevent unnecessary X-ray scattering in the camera. We had to remove and then put back the collimator each time we changed the IP. Therefore, we controlled the alignment of the diffractometer by primary beam intensity measurements with a scintillation counter after each evacuation of the camera with the IP inside it. The process can only affect the intensities of partial reflections at the starting angle of oscillation. Other details are given in Table 1.

Intensities read using a Fuji BAS-2500 scanner were transferred to the DIP-420 or DIP-3000 format of the MAC Science system and then the *DENZO* program (Otwinowski & Minor, 1997) was used for indexing. Also the program *VIIPP* (Zhurov, 1999) for integration of the IP data was designed by one of us (VVZ). It has wide graphic capabilities and permits the visualization of images, zooming, and two- and three-dimensional plotting of single peak areas (Fig. 1). A number of different choices for setting the integration area are possible. Background counts z at points (x, y) were approximated as $z = ax + by + c$, where a, b and c were fitted by the least-squares method using the points outside the integration area in the background area (Table 1). The graphic capabilities allow us to check each reflection and delete unreliable reflections. These capabilities of the program have considerably improved the accuracy of integration, especially for high-angle reflections.

In our particular case the orientation of the elliptical integration area was along the increasing $\sin\theta/\lambda$ directions, which are radial from the primary beam position. The length of the elliptical axis along $\sin\theta/\lambda$ depended upon the θ angle in accordance with $a + b\tan\theta$, where a and b are constants. The length of the perpendicular axis was constant. The integration area had to be relatively large (Table 1), because calculated peak positions, refined with *DENZO*, were not always accurate enough for very high-angle reflections with large $\alpha1/\alpha2$ separation. After the integration 20% of measured reflections had to be rejected because of the following reasons:

(i) Peaks with oscillation angles close to the starting positions of the φ rotation range showed extra high intensities owing to the preliminary beam-path test cited previously. Peaks close to end positions were often partially recorded. Therefore, reflections within 1° of the oscillation edges were deleted automatically.

(ii) For the reflections with positions close to 1° from the edges, the profile shape was the main criteria for rejection. We supposed that the intensity ratio for $\alpha2/\alpha1$ components of the peak had to be close to 1/2. Therefore, reflections with a $\alpha2/\alpha1$ ratio out of the range 1/3–2/3; were considered as partials and rejected. We also removed peaks with extra large intensities at several pixels (usually owing to scanner reading errors and cosmic rays).

Table 1. *Experimental details*

	IP	Four-circle
a (Å)	4.0110 (4)†	4.01082 (3)
Diffractometer	MAC Science rotating, anode generator λ = 0.71069 Å, graphite monochromator	
	V = 50 kV, I = 80 mA	V = 50 kV, I = 90 mA
Data collection method	φ rotation	Conventional
φ range (°)	0–186	
Oscillation step/overlapping (°)	16/6	
Integration area (mm)	$1.7 \times 1.7 + 0.7\tan\theta$	
Background area (mm)	$3.0 \times 3.0 + 0.7\tan\theta$	
$\omega/2\theta$ scan range (°)		$1.2 + 0.5\tan\theta$
$(\sin\theta/\lambda)_{max}$ (Å^{-1})	1.34	1.35
No of used reflections‡	2719	1328
No of independent reflections	144	166
$R_{int} = \Sigma(I_m - I_j)/\Sigma I_j$	0.0311	0.0245

† Measured routinely in a brief four-circle experiment. ‡ In the IP case some reflections were rejected (see text).

The subsequent scaling of the data was performed using the *SCALEPACK* program (Otwinowski & Minor, 1997). In the usual scaling process the presence of reflections with incorrect intensities may produce incorrect scale factors. To reduce these errors, we first scaled all 8 min images to the corresponding 2 h ones. Second we scaled all 2 h images to the first 2 h image with the oscillation range 0–16°. We thus obtained values for scaling all the images to the first 2 h image. The difference among these scale factors of the images measured with the same exposure time was less than 3%.

We also performed an accurate X-ray experiment with a conventional four-circle geometry. The details are given in Table 1. All reflections were measured with the same 2° min^{-1} speed in ω with up to 10 repetitions in order to measure intensities with 1.0% accuracy. The stability of the diffractometer was controlled by measuring the three reference reflections in orthogonal directions, 200, 020 and 002, after every 30 reflections. The maximum deviation of their intensities was less than 0.5%. A multiple diffraction effect was avoided by calculating the ψ-angle where the multiple diffraction effect can be neglected using the program *IUANGLE* (Tanaka *et al.*, 1994). Reflections in the region $2\theta = 0$–30° were measured in the reciprocal sphere. Only one reflection, for which multiple diffraction could not be avoided effectively, was removed afterwards. In $2\theta = 30$–150° mainly one octant of reciprocal space was

measured in order to spare experimental time. If a reflection in an octant could not be measured avoiding multiple diffraction, an actual equivalent reflection in the other octants was measured, as performed previously (Tanaka *et al.*, 1997).

All the data have been corrected for Lorentz–polarization factor, and absorption and thermal diffuse scattering (TDS) with the program *TDS*1&2*FF* (Tsarkov & Tsirelson, 1991); the maximum *TDS* correction was 15.4% for the $10,\bar{3}2$ reflection. Also, we had to correct our IP data for the oblique incidence (Tanaka *et al.*, 1999). The intensity of the oblique diffracted beam, measured by the scanner, is greater than that of the normal beam. It is a complex effect relating to the absorption of X-rays and emitted light from the scanner by a photoluminescent layer of Eu-doped BaFBr in the IP. When the absorption of irradiated light by the layer is dominantly greater than that of diffracted X-rays by the layer, the observed intensity $I_{\rm uncor}$ can be corrected for by $I_{\rm corr} = I_{\rm uncorr}\cos(\nu)$ (ν is an angle between the diffracted beam and that normal to the IP plane). It was up to 22% for the $\bar{2}82$ reflection intensity with $\nu = 39.2^\circ$.

Table 2. *Refinement results*

Models	Spherical		Aspherical	
Experiment	IP	Four-circle	IP	Four-circle
$y_{\rm min}$†	0.80	0.81	0.83	0.81
K^+				
U (Å)	0.01278 (9)	0.01251 (5)	0.0140 (3)	0.0129 (2)
q_{1111}			55 (8)	11 (6)
q_{1122}			6 (24)	26 (17)
Ni^+				
U (Å)	0.00566 (5)	0.00543 (3)	0.0070 (2)	0.0051 (4)
q_{1111}			300 (34)	−327 (275)
q_{1122}			278 (106)	436 (249)
F^-				
U^{11} (Å)	0.0062 (2)	0.0058 (1)	0.0085 (6)	0.0081 (3)
U^{22} (Å)	0.0158 (3)	0.0155 (2)	0.0180 (5)	0.0171 (3)
q_{1111}			360 (60)	329 (37)
q_{2222}			18 (81)	136 (46)
q_{1122}			38 (10)	15 (5)
q_{2233}			16 (34)	55 (21)
R	0.0139	0.0088	0.0073	0.0045
wR	0.0215	0.0144	0.0109	0.0055
k‡	0.0003	0.0001	0.0001	0.00001
S§	1.17	1.28	0.99	1.18

† Minimal extinction correction. ‡ k coefficient of weighting scheme: $w = 1/[\sigma^2(|F|) + k|F|^2]$. § Goodness-of-fit.

3. Refinement

Two different types of structure models have been considered: ionic spherical and aspherical. In order to compare the qualities of the IP and four-circle data, the refinement was performed in exactly the same way for both experiments (Table 2). For the least-squares refinement we used the ionic scattering factors for K^+ and F^- from the *International Tables for Crystallography* (1992, Vol. C). The program *QNTAO* (Tanaka,

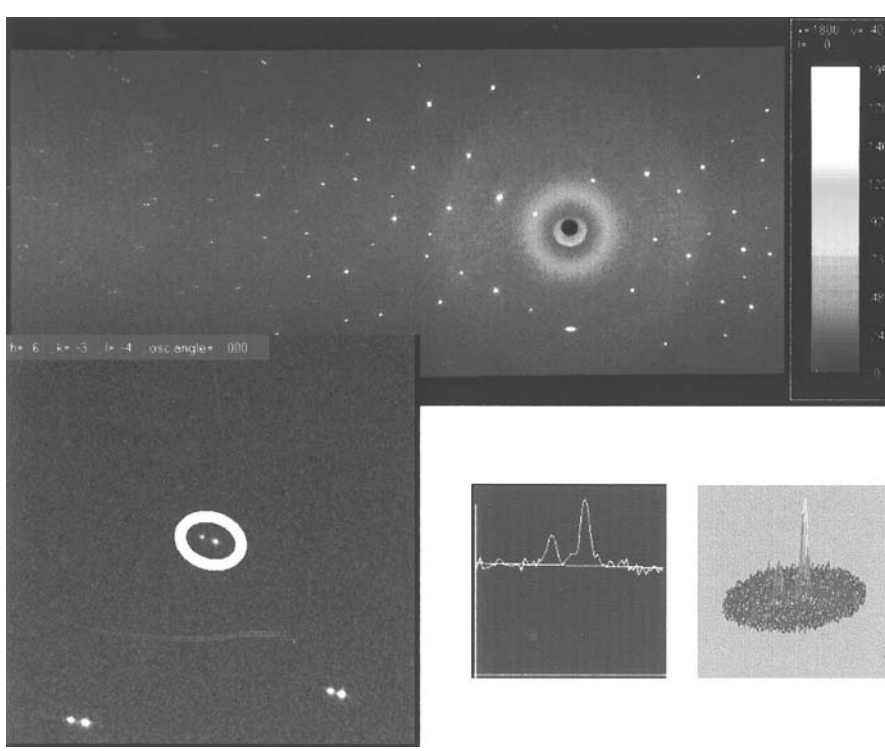

Fig. 1. Graphic capabilities of the *VIIPP* integration program.

1988), in which the aspherical electron distribution of atomic orbitals up to *f*-electrons can be treated, was used for the refinement. Statistical averaging methods (Dawson *et al.*, 1967; Tanaka & Marumo, 1983) for the treatment of anharmonicity of atomic vibrations and the type I extinction correction with an isotropic Gaussian distribution of mosaic spread (Becker & Coppens, 1974*a*,*b*) were applied in every case. Since the precise orientation of the crystal was not obtained in the present study for VCIP measurement, anisotropic extinction was not corrected for in both cases. The aspherical electronic structure of Ni^{2+} 3*d*-orbitals was taken into account by allotting six electrons on three t_{2g} orbitals and two on two e_g orbitals in a cubic O_h crystal field. Ar-core and *d*-orbital scattering factors for Ni^{2+} were obtained from the *International Tables for X-ray Crystallography* (1974, Vol. IV). The occupation numbers were fixed in the refinement. The final results were statistically correct according to the test of Abrahams & Keve (1971).

4. Results and discussion

The results are listed in Table 2.† The reliability factors and harmonic thermal parameters are systematically greater in the IP case. The maximal difference is 4% (8 e.s.d.s) for the nickel vibration parameter. The difference in anharmonic parameters, which probably accumulate all possible errors during the refinement process, is also significant. We suppose that the multiple diffraction effect is the main reason for this difference. In the present study the orientation matrix for the VCIP experiment, which is precise enough to make the detection of multiple diffraction possible, could not be obtained. A study to obtain the precise orientation of the crystal in the VCIP method is being undertaken, taking into account all the possible sources of displacement of peak positions.

The results of both refinements were used to calculate difference electron density ($\Delta\rho$) maps. The anomalous dispersion parts ($F_{obs} = F_{obs}^{anom}\ F_{calc}/F_{calc}^{anom}$) have been extracted from both F_{obs} and F_{calc}. The maps are shown in Fig. 2. We estimated the error level of $\Delta\rho$ in interatomic space to be $\sim$0.08 e Å^{-3}, which is typical in precise investigations of perovskite crystals (Zhurova *et al.*, 1995; Abramov *et al.*, 1995). Thus, only contours above this level are shown. The $\Delta\rho$ distributions are in good qualitative agreement with each other and with that published earlier (Kijima *et al.*, 1983). The $\Delta\rho$ map of the four-circle experiment (Fig. 2*b*) looks more 'clean'; the depths of the minima around the Ni atom are much less, but their positions at a distance of 0.4 Å from the Ni nuclei are the same. The resulting $\Delta\rho$ maps are shown in Fig. 3. $\Delta\rho$ peaks around the Ni atom practically disappear in both cases when asphericity is considered. This comparison shows that the IP experiment can be used effectively for electron density investigations.

Much work has been done in the treatment of IP data since it is the first precise IP investigation of inorganic compounds. For example, the rejection

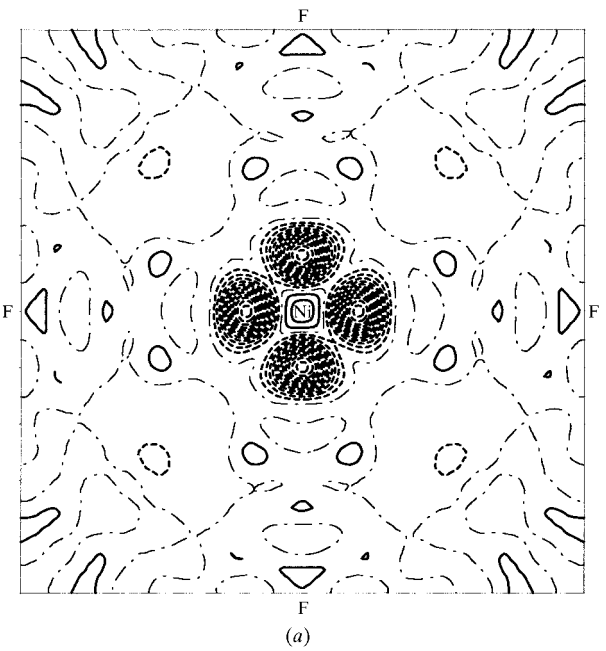

(*a*)

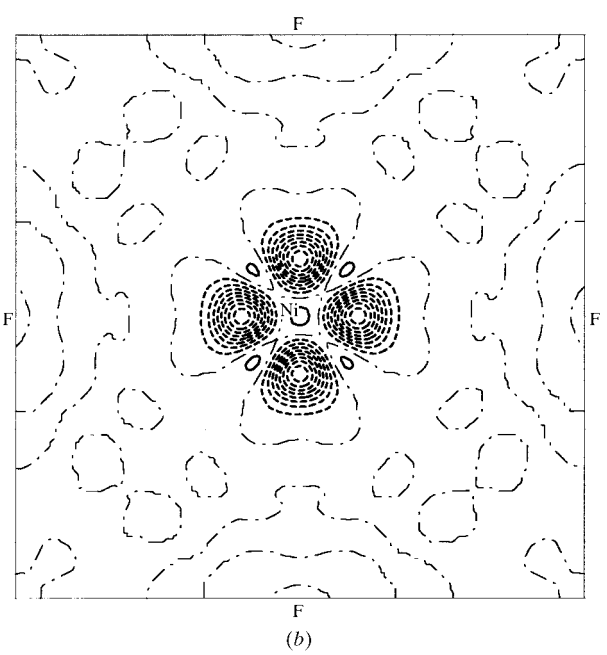

(*b*)

Fig. 2. $\Delta\rho$ maps after refinement of the spherical harmonic model. (*a*) IP and (*b*) four-circle experiments. Contour interval 0.1 e Å^{-3}. Positive contours are solid, negative ones are dashed and the zero level is dash-dotted.

† Supplementary data for this paper are available from the IUCr electronic archives (Reference: OA0022). Services for accessing these data are described at the back of the journal.

procedure of reflections in the present study may produce some bias during subsequent scaling, which consequently may produce a distortion in the refined structure model. Automatization of this process using numerical criteria of rejection assigned during this work will be performed in the near future.

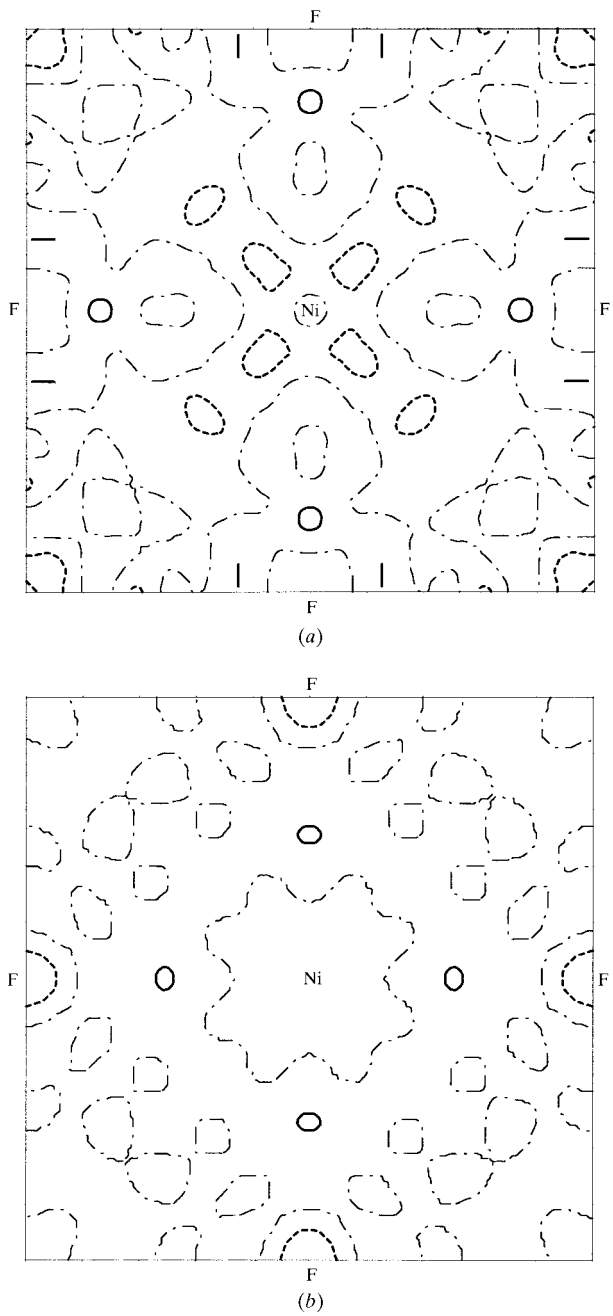

Fig. 3. $\Delta\rho$ map for the aspherical anharmonic model. (*a*) IP and (*b*) four-circle experiments. Contours as in Fig. 2.

5. Conclusion

In this work we demonstrate one of the significant problems of the IP method: low accuracy of data owing to the high background; this can be successfully solved using a vacuum camera. This method can obtain data with good precision within a few days, while it takes a couple of weeks to measure the same quality data with a scintillation detector. Although the statistical accuracy of the IP data was a little worse, it was good enough to reproduce qualitatively all the features of a precise electron density distribution experiment, even for the 3*d* shell of a Ni atom. The refinement of a complicated structure model, including the asphericity of the shell and the anharmonicity of atomic vibrations, was also successful for both cases. Our VCIP method can be very helpful for material science investigations and also for studies of non-stable compounds. Cooling of the sample, careful multiple diffraction analysis and further development of the integration procedure will improve the accuracy of the data further and improve times. This will be the subject of our next work.

Support of this work by CREST of JST is gratefully acknowledged. VVZ thanks the Russian Fund of Fundamental Research (grant No. 97–03-33776) for the financial support.

References

Abrahams, S. C. & Keve, E. T. (1971). *Acta Cryst.* A**27**, 157–165.
Abramov, Yu. A., Tsirelson, V. G., Zavodnik, V. E., Ivanov, S. A. & Brown, I. D. (1995). *Acta Cryst.* B**51**, 942–951.
Amemiya, Y. (1999). Private communication.
Amemiya, Y. & Miyahara, J. (1988). *Nature*, **336**, 89–90.
Becker, P. J. & Coppens, P. (1974*a*). *Acta Cryst.* A**30**, 129–147.
Becker, P. J. & Coppens, P. (1974*b*). *Acta Cryst.* A**30**, 148–153.
Bolotovsky, R., White, M. A., Darovsky, A. & Coppens, P. (1995). *J. Appl. Cryst.* **28**, 86–95.
Carducci, M. D., Pressprich, M. R. & Coppens, P. (1997). *J. Am. Chem. Soc.* **119**, 2669–2678.
Darovsky, A. & Coppens, P. (1998). *J. Appl. Cryst.* **31**, 296–298.
Dawson, B., Hurley, A. C. & Maslen, V. W. (1967). *Proc. R. Soc. London Ser. A*, **298**, 289–306.
Iversen, B., Darovsky, A., Bolotovsky, R. & Coppens, P. (1998). *Acta Cryst.* B**54**, 174–179.
Iwasaki, F., Sakuratani, M., Kaneko, H., Yasui, M., Kamiya, N. & Iwasaki, H. (1995). *Acta Cryst.* B**51**, 1028–1035.
Kijima, N., Tanaka, K. & Marumo, F. (1983). *Acta Cryst.* B**39**, 557–561.
Ohsumi, K., Hagiya, K. & Ohmasa, M. (1991). *J. Appl. Cryst.* **24**, 340–348.
Ohsumi, K., Hagiya, K., Uchida, M., Suda, N., Miyamoto, M., Kitamura, M. & Ohmasa, M. (1995). *Rev. Sci. Instrum.* **66**, 1448–1450.
Otwinowski, Z. & Minor, W. (1997). *Methods Enzymol. A*, **276**, 307–326.
Sakabe, N. (1991). *Nucl. Instrum. Methods Phys. Res. A*, **303**, 448–463.

Tanaka, K. (1988). *Acta Cryst.* A**44**, 1002–1008.
Tanaka, K., Kato, Y. & Onuki, Y. (1997). *Acta Cryst.* B**53**, 143–152.
Tanaka, K., Kumazawa, S., Tsubokawa, M., Maruno, S. & Shirotani, I. (1994). *Acta Cryst.* A**50**, 246–252.
Tanaka, K. & Marumo, F. (1983). *Acta Cryst.* A**39**, 631–641.
Tanaka, K., Zhurova, E. A., Zhurov, V. V. & Kitamura, S. (1999). *J. Appl. Cryst.* In preparation.
Tsarkov, A. G. & Tsirelson, V. G. (1991). *Phys. Status Solidi B*, **167**, 417–428.
Zhurov, V. V. (1999). To be published.
Zhurova, E. A., Zavodnik, V. E. & Tsirelson, V. G. (1995). *Crystallogr. Rep.* **40**, 816–823.